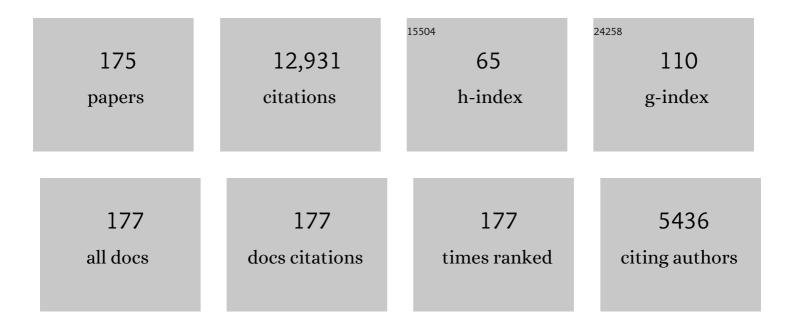
## Larry Nittler

List of Publications by Year in descending order

Source: https://exaly.com/author-pdf/4929604/publications.pdf Version: 2024-02-01



LADDY NITTLED

#	Article	IF	CITATIONS
1	Samples returned from the asteroid Ryugu are similar to Ivuna-type carbonaceous meteorites. Science, 2023, 379, .	12.6	97
2	MESSENGER Xâ€Ray Observations of Electron Precipitation on the Dayside of Mercury. Journal of Geophysical Research: Space Physics, 2022, 127, .	2.4	8
3	Organic synthesis associated with serpentinization and carbonation on early Mars. Science, 2022, 375, 172-177.	12.6	32
4	Pebbles and sand on asteroid (162173) Ryugu: In situ observation and particles returned to Earth. Science, 2022, 375, 1011-1016.	12.6	78
5	Cluster Analysis of Presolar Silicon Carbide Grains: Evaluation of Their Classification and Astrophysical Implications. Astrophysical Journal Letters, 2021, 907, L39.	8.3	18
6	Presolar stardust in highly pristine CM chondrites Asuka 12169 and Asuka 12236. Meteoritics and Planetary Science, 2021, 56, 260-276.	1.6	17
7	TEM Analyses of Unusual Presolar Silicon Carbide: Insights into the Range of Circumstellar Dust Condensation Conditions. Astrophysical Journal, 2021, 913, 90.	4.5	7
8	Highly volatile element (H, C, F, Cl, S) abundances and H isotopic compositions in chondrules from carbonaceous and ordinary chondrites. Geochimica Et Cosmochimica Acta, 2021, 301, 230-258.	3.9	13
9	Record of Alteration by Heavy Ices in a Cometary Clast in a Primitive Meteorite. Microscopy and Microanalysis, 2021, 27, 2268-2270.	0.4	0
10	The Distribution of Peakâ€Ring Basins on Mercury and Their Correlation With the Highâ€Mg/Si Terrane. Journal of Geophysical Research E: Planets, 2021, 126, e2021JE006839.	3.6	2
11	New Multielement Isotopic Compositions of Presolar SiC Grains: Implications for Their Stellar Origins. Astrophysical Journal Letters, 2021, 920, L26.	8.3	10
12	Evaluation of the classification of pre-solar silicon carbide grains using consensus clustering with resampling methods: An assessment of the confidence of grain assignments. Monthly Notices of the Royal Astronomical Society, 2021, 510, 334-350.	4.4	10
13	Effects of aqueous alteration on primordial noble gases and presolar SiC in the carbonaceous chondrite Tagish Lake. Meteoritics and Planetary Science, 2020, 55, 1257-1280.	1.6	4
14	Presolar grains in primitive ungrouped carbonaceous chondrite Northwest Africa 5958. Meteoritics and Planetary Science, 2020, 55, 1160-1175.	1.6	13
15	Coordinated EDX and microâ€Raman analysis of presolar silicon carbide: A novel, nondestructive method to identify rare subgroup SiC. Meteoritics and Planetary Science, 2020, 55, .	1.6	0
16	Abundant extraterrestrial amino acids in the primitive CM carbonaceous chondrite Asuka 12236. Meteoritics and Planetary Science, 2020, 55, 1979-2006.	1.6	38
17	The BepiColombo Mercury Imaging X-Ray Spectrometer: Science Goals, Instrument Performance and Operations. Space Science Reviews, 2020, 216, 1.	8.1	36
18	Sampling interplanetary dust from Antarctic air. Meteoritics and Planetary Science, 2020, 55, 1128-1145.	1.6	4

#	Article	IF	CITATIONS
19	Rationale for BepiColombo Studies of Mercury's Surface and Composition. Space Science Reviews, 2020, 216, 1.	8.1	46
20	Global major-element maps of Mercury from four years of MESSENGER X-Ray Spectrometer observations. Icarus, 2020, 345, 113716.	2.5	27
21	No FeS layer in Mercury? Evidence from Ti/Al measured by MESSENGER. Earth and Planetary Science Letters, 2020, 534, 116108.	4.4	19
22	Origin of Large Meteoritic SiC Stardust Grains in Metal-rich AGB Stars. Astrophysical Journal, 2020, 898, 96.	4.5	21
23	Microscale Hydrogen and Nitrogen Isotopic Distributions in Pristine CM Chondrite Asuka 12236. , 2020, , .		1
24	Reply to: GEMS and the devil in their details. Nature Astronomy, 2019, 3, 606-606.	10.1	2
25	Presolar Silicon Carbide Grains of Types Y and Z: Their Molybdenum Isotopic Compositions and Stellar Origins. Astrophysical Journal, 2019, 881, 28.	4.5	23
26	Re-examining thermal metamorphism of the Renazzo-like (CR) carbonaceous chondrites: Insights from pristine Miller Range 090657 and shock-heated Graves Nunataks 06100. Geochimica Et Cosmochimica Acta, 2019, 267, 240-256.	3.9	16
27	Mineralogy and petrology of Dominion Range 08006: A very primitive CO3 carbonaceous chondrite. Geochimica Et Cosmochimica Acta, 2019, 265, 259-278.	3.9	42
28	The Surface Composition of Mercury. Elements, 2019, 15, 33-38.	0.5	28
29	A cometary building block in a primitive asteroidal meteorite. Nature Astronomy, 2019, 3, 659-666.	10.1	73
30	Fossil biomass preserved as graphitic carbon in a late Paleoproterozoic banded iron formation metamorphosed at more than 550°C. Journal of the Geological Society, 2019, 176, 651-668.	2.1	5
31	Remnants and ejecta of thermonuclear electron-capture supernovae. Astronomy and Astrophysics, 2019, 622, A74.	5.1	47
32	High abundances of presolar grains and 15N-rich organic matter in CO3.0 chondrite Dominion Range 08006. Geochimica Et Cosmochimica Acta, 2018, 226, 107-131.	3.9	42
33	Late formation of silicon carbide in type II supernovae. Science Advances, 2018, 4, eaao1054.	10.3	29
34	Extremely <sup>54</sup> Cr- and <sup>50</sup> Ti-rich Presolar Oxide Grains in a Primitive Meteorite: Formation in Rare Types of Supernovae and Implications for the Astrophysical Context of Solar System Birth. Astrophysical Journal Letters, 2018, 856, L24.	8.3	48
35	Correlated XANES, TEM, and NanoSIMS of presolar graphite grains. Geochimica Et Cosmochimica Acta, 2018, 221, 219-236.	3.9	10
36	Titanium isotopic compositions of rare presolar SiC grain types from the Murchison meteorite. Geochimica Et Cosmochimica Acta, 2018, 221, 162-181.	3.9	15

#	Article	IF	CITATIONS
37	Bonanza: An extremely large dust grain from a supernova. Geochimica Et Cosmochimica Acta, 2018, 221, 60-86.	3.9	34
38	New Constraints on the Major Neutron Source in Low-mass AGB Stars. Astrophysical Journal, 2018, 865, 112.	4.5	29
39	The MESSENGER Mission: Science and Implementation Overview. , 2018, , 1-29.		10
40	The Chemical Composition of Mercury. , 2018, , 30-51.		43
41	Mercury's Crust and Lithosphere: Structure and Mechanics. , 2018, , 52-84.		9
42	Mercury's Internal Structure. , 2018, , 85-113.		26
43	The Geologic History of Mercury. , 2018, , 144-175.		10
44	The Geochemical and Mineralogical Diversity of Mercury. , 2018, , 176-190.		21
45	Spectral Reflectance Constraints on the Composition and Evolution of Mercury's Surface. , 2018, , 191-216.		9
46	Impact Cratering of Mercury. , 2018, , 217-248.		10
47	The Volcanic Character of Mercury. , 2018, , 287-323.		13
48	Mercury's Hollows. , 2018, , 324-345.		12
49	Mercury's Polar Deposits. , 2018, , 346-370.		9
50	Observations of Mercury's Exosphere: Composition and Structure. , 2018, , 371-406.		5
51	Understanding Mercury's Exosphere: Models Derived from MESSENGER Observations. , 2018, , 407-429.		8
52	Mercury's Dynamic Magnetosphere. , 2018, , 461-496.		8
53	The Elusive Origin of Mercury. , 2018, , 497-515.		21
54	High-temperature Dust Condensation around an AGB Star: Evidence from a Highly Pristine Presolar Corundum. Astrophysical Journal Letters, 2018, 862, L13.	8.3	17

#	Article	IF	CITATIONS
55	Low Energy STEM-EELS Characterization of Primitive Organic Matter and Silicates in the Meteorite LAP 02342. Microscopy and Microanalysis, 2018, 24, 2074-2075.	0.4	1
56	Common Occurrence of Explosive Hydrogen Burning in Type II Supernovae. Astrophysical Journal, 2018, 855, 144.	4.5	15
57	Evidence Connecting Mercury's Magnesium Exosphere to Its Magnesiumâ€Rich Surface Terrane. Geophysical Research Letters, 2018, 45, 6790-6797.	4.0	21
58	Origin of meteoritic stardust unveiled by a revised proton-capture rate of 170. Nature Astronomy, 2017, 1, .	10.1	64
59	The nature, origin and modification of insoluble organic matter in chondrites, the major source of Earth's C and N. Chemie Der Erde, 2017, 77, 227-256.	2.0	163
60	Evaluating an impact origin for Mercury's high-magnesium region. Journal of Geophysical Research E: Planets, 2017, 122, 614-632.	3.6	19
61	Geochemistry, mineralogy, and petrology of boninitic and komatiitic rocks on the mercurian surface: Insights into the mercurian mantle. Icarus, 2017, 285, 155-168.	2.5	79
62	A Low O/Si Ratio on the Surface of Mercury: Evidence for Silicon Smelting?. Journal of Geophysical Research E: Planets, 2017, 122, 2053-2076.	3.6	36
63	Coordinated <scp>EDX</scp> and microâ€Raman analysis of presolar silicon carbide: A novel, nondestructive method to identify rare subgroup SiC. Meteoritics and Planetary Science, 2017, 52, 2550-2569.	1.6	16
64	J-type Carbon Stars: A Dominant Source of <sup>14</sup> N-rich Presolar SiC Grains of Type AB. Astrophysical Journal Letters, 2017, 844, L12.	8.3	25
65	Evidence for Reduced, Carbon-rich Regions in the Solar Nebula from an Unusual Cometary Dust Particle. Astrophysical Journal, 2017, 848, 113.	4.5	7
66	The future of Stardust science. Meteoritics and Planetary Science, 2017, 52, 1859-1898.	1.6	16
67	Compositional terranes on Mercury: Information from fast neutrons. Icarus, 2017, 281, 32-45.	2.5	30
68	Determining the Elemental and Isotopic Composition of the Pre-solar Nebula from Genesis Data Analysis: The Case of Oxygen. Astrophysical Journal Letters, 2017, 851, L12.	8.3	15
69	Measuring the level of interstellar inheritance in the solar protoplanetary disk. Meteoritics and Planetary Science, 2017, 52, 1797-1821.	1.6	39
70	Stellar Origin of <sup>15</sup> N-rich Presolar SiC Grains of Type AB: Supernovae with Explosive Hydrogen Burning. Astrophysical Journal Letters, 2017, 842, L1.	8.3	55
71	Ernst K. Zinner (1937–2015). , 2017, , .		0
72	Meteoritic Stardust and the Presolar History of the Solar Neighborhood. , 2017, , .		0

#	Article	IF	CITATIONS
73	Astrophysics with Extraterrestrial Materials. Annual Review of Astronomy and Astrophysics, 2016, 54, 53-93.	24.3	133
74	Evidence from MESSENGER for sulfur―and carbonâ€driven explosive volcanism on Mercury. Geophysical Research Letters, 2016, 43, 3653-3661.	4.0	57
75	STELLAR ORIGINS OF EXTREMELY <sup>13</sup> C- AND <sup>15</sup> N-ENRICHED PRESOLAR SIC GRAINS: NOVAE OR SUPERNOVAE?. Astrophysical Journal, 2016, 820, 140.	4.5	51
76	Calibration of the MESSENGER X-Ray Spectrometer. Planetary and Space Science, 2016, 122, 13-25.	1.7	5
77	Remote sensing evidence for an ancient carbon-bearing crust on Mercury. Nature Geoscience, 2016, 9, 273-276.	12.9	134
78	INFERRED INITIAL <sup>26</sup> Al/ <sup>27</sup> Al RATIOS IN PRESOLAR STARDUST GRAINS FROM SUPERNOVAE ARE HIGHER THAN PREVIOUSLY ESTIMATED. Astrophysical Journal, 2015, 809, 31.	4.5	29
79	Ion Implants as Matrixâ€Appropriate Calibrators for Geochemical Ion Probe Analyses. Geostandards and Geoanalytical Research, 2015, 39, 265-276.	3.1	18
80	Geochemical terranes of Mercury's northern hemisphere as revealed by MESSENGER neutron measurements. Icarus, 2015, 253, 346-363.	2.5	74
81	Constraints on the abundance of carbon in near-surface materials on Mercury: Results from the MESSENGER Gamma-Ray Spectrometer. Planetary and Space Science, 2015, 108, 98-107.	1.7	57
82	Evidence for geochemical terranes on Mercury: Global mapping of major elements with MESSENGER's X-Ray Spectrometer. Earth and Planetary Science Letters, 2015, 416, 109-120.	4.4	167
83	Chlorine on the surface of Mercury: MESSENGER gamma-ray measurements and implications for the planet's formation and evolution. Icarus, 2015, 257, 417-427.	2.5	66
84	Orbital multispectral mapping of Mercury with the MESSENGER Mercury Dual Imaging System: Evidence for the origins of plains units and low-reflectance material. Icarus, 2015, 254, 287-305.	2.5	95
85	Hydrogen and major element concentrations on 433 Eros: Evidence for an L―or <scp>LL</scp> â€chondriteâ€like surface composition. Meteoritics and Planetary Science, 2015, 50, 353-367.	1.6	30
86	SOLAR FLARE ELEMENT ABUNDANCES FROM THE SOLAR ASSEMBLY FOR X-RAYS (SAX) ON <i>MESSENGER</i> . Astrophysical Journal, 2015, 803, 67.	4.5	30
87	Elemental, isotopic, and structural changes in Tagish Lake insoluble organic matter produced by parent body processes. Meteoritics and Planetary Science, 2014, 49, 503-525.	1.6	75
88	Abundances of presolar silicon carbide grains in primitive meteorites determined by NanoSIMS. Geochimica Et Cosmochimica Acta, 2014, 139, 248-266.	3.9	80
89	Enhanced sodium abundance in Mercury's north polar region revealed by the MESSENGER Gamma-Ray Spectrometer. Icarus, 2014, 228, 86-95.	2.5	85
90	Stardust Interstellar Preliminary Examination V: <scp>XRF</scp> analyses of interstellar dust candidates at <scp>ESRF ID</scp> 13. Meteoritics and Planetary Science, 2014, 49, 1594-1611.	1.6	12

#	Article	IF	CITATIONS
91	Fluid-induced organic synthesis in the solar nebula recorded in extraterrestrial dust from meteorites. Proceedings of the National Academy of Sciences of the United States of America, 2014, 111, 15338-15343.	7.1	29
92	Stardust Interstellar Preliminary Examination <scp>III</scp> : Infrared spectroscopic analysis of interstellar dust candidates. Meteoritics and Planetary Science, 2014, 49, 1548-1561.	1.6	12
93	Evidence for interstellar origin of seven dust particles collected by the Stardust spacecraft. Science, 2014, 345, 786-791.	12.6	152
94	Mercury's Weather-Beaten Surface: Understanding Mercury in the Context of Lunar and Asteroidal Space Weathering Studies. Space Science Reviews, 2014, 181, 121-214.	8.1	108
95	A transmission electron microscopy study of presolar spinel. Geochimica Et Cosmochimica Acta, 2014, 124, 152-169.	3.9	29
96	Variations in the abundance of iron on Mercury's surface from MESSENGER X-Ray Spectrometer observations. Icarus, 2014, 235, 170-186.	2.5	93
97	3D Nanoscale Analysis Using Focused Ion Beam Tomography of Carbonaceous Nanoglobules in Matrix Materials from the Tagish Lake Meterorite. Microscopy and Microanalysis, 2014, 20, 318-319.	0.4	0
98	Coordinated Electron and X-ray Microscopy of Cometary Organic Matter Collected by the NASA Stardust Mission Microscopy and Microanalysis, 2014, 20, 1694-1695.	0.4	1
99	Morphologies, Isotopes, Crystal Structures, and Microstructures of Presolar Al2O3 Grains: a NanoSIMS, EBSD, EDS, CL, and FIB-TEM study. Microscopy and Microanalysis, 2014, 20, 1696-1697.	0.4	0
100	Determination of the Effects of Hydrothermal Alteration on Silicate Stardust with Secondary Ion Mass Spectrometry and Transmission Electron Microscopy. Microscopy and Microanalysis, 2014, 20, 1698-1699.	0.4	0
101	Evidence for Water Ice Near Mercury's North Pole from MESSENGER Neutron Spectrometer Measurements. Science, 2013, 339, 292-296.	12.6	173
102	Isotopic and chemical variation of organic nanoglobules in primitive meteorites. Meteoritics and Planetary Science, 2013, 48, 904-928.	1.6	78
103	The redox state, FeO content, and origin of sulfurâ€rich magmas on Mercury. Journal of Geophysical Research E: Planets, 2013, 118, 138-146.	3.6	112
104	Magnesiumâ€rich crustal compositions on Mercury: Implications for magmatism from petrologic modeling. Journal of Geophysical Research, 2012, 117, .	3.3	83
105	Galactic chemical evolution and the oxygen isotopic composition of the solar system. Meteoritics and Planetary Science, 2012, 47, 2031-2048.	1.6	23
106	MESSENGER detection of electronâ€induced Xâ€ray fluorescence from Mercury's surface. Journal of Geophysical Research, 2012, 117, .	3.3	46
107	Variations in the abundances of potassium and thorium on the surface of Mercury: Results from the MESSENGER Gammaâ€Ray Spectrometer. Journal of Geophysical Research, 2012, 117, .	3.3	85
108	Chemical heterogeneity on Mercury's surface revealed by the MESSENGER Xâ€Ray Spectrometer. Journal of Geophysical Research, 2012, 117, .	3.3	144

#	Article	IF	CITATIONS
109	Majorâ€element abundances on the surface of Mercury: Results from the MESSENGER Gammaâ€Ray Spectrometer. Journal of Geophysical Research, 2012, 117, .	3.3	146
110	Aluminum abundance on the surface of Mercury: Application of a new backgroundâ€reduction technique for the analysis of gammaâ€ray spectroscopy data. Journal of Geophysical Research, 2012, 117, .	3.3	23
111	The Provenances of Asteroids, and Their Contributions to the Volatile Inventories of the Terrestrial Planets. Science, 2012, 337, 721-723.	12.6	511
112	Hollows on Mercury: MESSENGER Evidence for Geologically Recent Volatile-Related Activity. Science, 2011, 333, 1856-1859.	12.6	136
113	Raman Spectroscopy on Cometary and Meteoritic Organic Matter. Spectroscopy Letters, 2011, 44, 554-559.	1.0	2
114	The Major-Element Composition of Mercury's Surface from MESSENGER X-ray Spectrometry. Science, 2011, 333, 1847-1850.	12.6	386
115	Radioactive Elements on Mercury's Surface from MESSENGER: Implications for the Planet's Formation and Evolution. Science, 2011, 333, 1850-1852.	12.6	233
116	Flood Volcanism in the Northern High Latitudes of Mercury Revealed by MESSENGER. Science, 2011, 333, 1853-1856.	12.6	225
117	Correlated microanalysis of cometary organic grains returned by Stardust. Meteoritics and Planetary Science, 2011, 46, 1376-1396.	1.6	53
118	Origin and Evolution of Prebiotic Organic Matter As Inferred from the Tagish Lake Meteorite. Science, 2011, 332, 1304-1307.	12.6	189
119	A TRANSMISSION ELECTRON MICROSCOPY STUDY OF PRESOLAR HIBONITE. Astrophysical Journal, 2011, 730, 83.	4.5	23
120	Observations of suprathermal electrons in Mercury's magnetosphere during the three MESSENGER flybys. Planetary and Space Science, 2011, 59, 2016-2025.	1.7	31
121	Establishing a molecular relationship between chondritic and cometary organic solids. Proceedings of the National Academy of Sciences of the United States of America, 2011, 108, 19171-19176.	7.1	181
122	AUTOMATED NanoSIMS MEASUREMENTS OF SPINEL STARDUST FROM THE MURRAY METEORITE. Astrophysical Journal, 2010, 717, 107-120.	4.5	64
123	Identification and measurement of neutron-absorbing elements on Mercury's surface. Icarus, 2010, 209, 195-209.	2.5	52
124	COORDINATED ANALYSES OF PRESOLAR GRAINS IN THE ALLAN HILLS 77307 AND QUEEN ELIZABETH RANGE 99177 METEORITES. Astrophysical Journal, 2010, 719, 166-189.	4.5	113
125	Isotopic anomalies in organic nanoglobules from Comet 81P/Wild 2: Comparison to Murchison nanoglobules and isotopic anomalies induced in terrestrial organics by electron irradiation. Geochimica Et Cosmochimica Acta, 2010, 74, 4454-4470.	3.9	100
126	Evidence for extended acceleration of solar flare ions from 1–8 MeV solar neutrons detected with the MESSENGER Neutron Spectrometer. Journal of Geophysical Research, 2010, 115, .	3.3	26

#	Article	IF	CITATIONS
127	Properties and distribution of paired candidate stony meteorites at Meridiani Planum, Mars. Journal of Geophysical Research, 2010, 115, .	3.3	19
128	Mineral associations and character of isotopically anomalous organic material in the Tagish Lake carbonaceous chondrite. Geochimica Et Cosmochimica Acta, 2010, 74, 5966-5983.	3.9	40
129	Cometary Dust in the Laboratory. Science, 2010, 328, 698-699.	12.6	8
130	Elemental composition of 433 Eros: New calibration of the NEAR-Shoemaker XRS data. Icarus, 2009, 200, 129-146.	2.5	45
131	Ultra-primitive interplanetary dust particles from the comet 26P/Grigg–Skjellerup dust stream collection. Earth and Planetary Science Letters, 2009, 288, 44-57.	4.4	187
132	On the Mass and Metallicity Distributions of the Parent AGB Stars of O-Rich Presolar Stardust Grains. Publications of the Astronomical Society of Australia, 2009, 26, 271-277.	3.4	40
133	Meteorites on Mars observed with the Mars Exploration Rovers. Journal of Geophysical Research, 2008, 113, .	3.3	75
134	Combined microâ€Raman, microâ€infrared, and field emission scanning electron microscope analyses of comet 81P/Wild 2 particles collected by Stardust. Meteoritics and Planetary Science, 2008, 43, 367-397.	1.6	89
135	Mercury's Magnetosphere After MESSENGER's First Flyby. Science, 2008, 321, 85-89.	12.6	166
136	Presolar Stardust in the Solar System: Implications for Nucleosynthesis and Galactic Chemical Evolution. AIP Conference Proceedings, 2008, , .	0.4	0
137	Structural, chemical and isotopic examinations of interstellar organic matter extracted from meteorites and interstellar dust particles. Proceedings of the International Astronomical Union, 2008, 4, 333-334.	0.0	0
138	Presolar grains in the Solar System: Connections to stellar and interstellar organics. Proceedings of the International Astronomical Union, 2008, 4, 343-344.	0.0	0
139	Aluminumâ€; Calcium―and Titaniumâ€rich Oxide Stardust in Ordinary Chondrite Meteorites. Astrophysical Journal, 2008, 682, 1450-1478.	4.5	163
140	4. Nucleosynthesis and Chemical Evolution of Oxygen. , 2008, , 31-54.		5
141	Characterization of Presolar Silicate and Oxide Grains in Primitive Carbonaceous Chondrites. Astrophysical Journal, 2007, 656, 1223-1240.	4.5	136
142	NanoSIMS isotopic analysis of small presolar grains: Search for Si3N4 grains from AGB stars and Al and Ti isotopic compositions of rare presolar SiC grains. Geochimica Et Cosmochimica Acta, 2007, 71, 4786-4813.	3.9	91
143	Coordinated isotopic and mineralogic analyses of planetary materials enabled by in situ liftâ€out with a focused ion beam scanning electron microscope. Meteoritics and Planetary Science, 2007, 42, 1373-1386.	1.6	74
144	Characterization of insoluble organic matter in primitive meteorites by microRaman spectroscopy. Meteoritics and Planetary Science, 2007, 42, 1387-1416.	1.6	264

#	Article	IF	CITATIONS
145	Comet 81P/Wild 2 Under a Microscope. Science, 2006, 314, 1711-1716.	12.6	848
146	Interstellar Chemistry Recorded in Organic Matter from Primitive Meteorites. Science, 2006, 312, 727-730.	12.6	315
147	Organics Captured from Comet 81P/Wild 2 by the Stardust Spacecraft. Science, 2006, 314, 1720-1724.	12.6	519
148	Silicon and Carbon Isotopic Ratios in AGB Stars: SiC Grain Data, Models, and the Galactic Evolution of the Si Isotopes. Astrophysical Journal, 2006, 650, 350-373.	4.5	125
149	Isotopic Compositions of Cometary Matter Returned by Stardust. Science, 2006, 314, 1724-1728.	12.6	343
150	Constraints on Heterogeneous Galactic Chemical Evolution from Meteoritic Stardust. Astrophysical Journal, 2005, 618, 281-296.	4.5	53
151	Are Presolar Silicon Carbide Grains from Novae Actually from Supernovae?. Astrophysical Journal, 2005, 631, L89-L92.	4.5	100
152	Oxygen, magnesium and chromium isotopic ratios of presolar spinel grains. Geochimica Et Cosmochimica Acta, 2005, 69, 4149-4165.	3.9	91
153	ASTRONOMY: Nuclear Fossils in Stardust. Science, 2004, 303, 636-637.	12.6	1
154	Polymorphism in Presolar Al2O3 Grains from Asymptotic Giant Branch Stars. Science, 2004, 305, 1455-1457.	12.6	90
155	Astrophysics with Presolar Stardust. Annual Review of Astronomy and Astrophysics, 2004, 42, 39-78.	24.3	257
156	Automated isotopic measurements of micron-sized dust: application to meteoritic presolar silicon carbide. Geochimica Et Cosmochimica Acta, 2003, 67, 4961-4980.	3.9	96
157	Presolar stardust in meteorites: recent advances and scientific frontiers. Earth and Planetary Science Letters, 2003, 209, 259-273.	4.4	175
158	Spectra of extremely reduced assemblages: Implications for Mercury. Meteoritics and Planetary Science, 2002, 37, 1233-1244.	1.6	108
159	Electron Microscopy of In Situ Presolar Silicon Carbide. Microscopy and Microanalysis, 2002, 8, 1550-1551.	0.4	3
160	The NEARâ€Shoemaker xâ€ray/gammaâ€ray spectrometer experiment: Overview and lessons learned. Meteoritics and Planetary Science, 2001, 36, 1605-1616.	1.6	19
161	Elemental composition from gammaâ€ray spectroscopy of the NEARâ€6hoemaker landing site on 433 Eros. Meteoritics and Planetary Science, 2001, 36, 1639-1660.	1.6	58
162	The composition of 433 Eros: A mineralogical—chemical synthesis. Meteoritics and Planetary Science, 2001, 36, 1661-1672.	1.6	93

#	Article	IF	CITATIONS
163	Xâ€ray fluorescence measurements of the surface elemental composition of asteroid 433 Eros. Meteoritics and Planetary Science, 2001, 36, 1673-1695.	1.6	110
164	Presolar SiC Grains of Type A and B: Their Isotopic Compositions and Stellar Origins. Astrophysical Journal, 2001, 559, 463-483.	4.5	136
165	Presolar Grains from Novae. Astrophysical Journal, 2001, 551, 1065-1072.	4.5	185
166	Presolar SiC Grains of Type Y: Origin from Lowâ€Metallicity Asymptotic Giant Branch Stars. Astrophysical Journal, 2001, 546, 248-266.	4.5	107
167	The Elemental Composition of Asteroid 433 Eros: Results of the NEAR-Shoemaker X-ray Spectrometer. Science, 2000, 289, 2101-2105.	12.6	123
168	The Galactic Evolution of Si, Ti, and O Isotopic Ratios. Astrophysical Journal, 1999, 519, 222-235.	4.5	71
169	Meteoritic oxide grain from supernova found. Nature, 1998, 393, 222-222.	27.8	86
170	Galactic Age Estimates from O-rich Stardust in Meteorites. Physical Review Letters, 1997, 78, 175-178.	7.8	35
171	Presolar oxide grains in meteorites. , 1997, , .		37
172	Stellar Sapphires: The Properties and Origins of Presolar Al2O3in Meteorites. Astrophysical Journal, 1997, 483, 475-495.	4.5	337
173	Extinct <sup>44</sup> Ti in Presolar Graphite and SiC: Proof of a Supernova Origin. Astrophysical Journal, 1996, 462, L31-L34.	4.5	146
174	Oxygen-rich stardust in meteorites. AIP Conference Proceedings, 1995, , .	0.4	13
175	Interstellar oxide grains from the Tieschitz ordinary chondrite. Nature, 1994, 370, 443-446.	27.8	213